Journal of Zhejiang University SCIENCE A
ISSN 1673-565X (Print); ISSN 1862-1775 (Online)
www.zju.edu.cn/jzus; www.springerlink.com
E-mail: jzus@zju.edu.cn

New analytical solution for the analysis and design of permanent magnet thrust bearings*

Huan YANG†, Rong-xiang ZHAO†‡, Shi-you YANG

(*School of Electrical Engineering, Zhejiang University, Hangzhou 310027, China*)

†E-mail: {k-night, rongxiang}@zju.edu.cn

Received July 8, 2008; Revision accepted Oct. 29, 2008; Crosschecked Apr. 27, 2009

Abstract: On the basis of the current sheet model, a new analytical solution for permanent magnet (PM) bearings is developed. Compared with analytical methods based on the coupling energy model and the magnetic dipole model, the proposed one is more physically intuitive and convenient for engineering designers. According to the analytical model, the thrust characteristics of a novel PM thrust bearing is studied and verified by finite element analysis (FEA). In the proposed thrust bearing configuration, the rotor is composed of stacked PM rings with alternative axial magnetization directions, and the stator with alternative radial magnetization directions while copper rings are used to separate adjacent PM rings. A prototype PM thrust bearing with the proposed configuration is designed and fabricated. The performances of the PM thrust bearing are experimentally validated. It is shown that the calculation accuracy of the presented analytical solution is satisfying.

Key words: Permanent magnet (PM), Current sheet model, Thrust bearing, Vibration
doi:10.1631/jzus.A0820520 **Document code:** A **CLC number:** TM153

INTRODUCTION

Permanent magnet (PM) bearings have attracted increasing attention from fellow researchers due to the advantages of PM. Most researchers have focused their studies on radial PM bearings (Mukhopadhyay *et al.*, 2000) and hybrid magnetic bearings (Xu *et al.*, 2006), while PM thrust bearings are also widely used in applications, such as the support of hydrogenerator rotors, the levitation of flywheels.

Obviously, a lot of geometric parameters and constraints need to be decided on when one designs a PM bearing. The implementation of finite element analysis (FEA) in such a PM bearing will become impractical because so many parameters are involved, and thus analytical solutions are required (Bancel and Lemarquand, 1998). The coupling energy model (Yonnet, 1981) and the magnetic charge model (Bancel and Lemarquand, 1998) have been used in the magnetic force or magnetic field analysis of PM rings or arrays. According to a comparison of five traditional mathematical models of PM bearings (Sun *et al.*, 2005), the magnetic charge model seems better than the others. However, the five mathematical models all involve complicated and iterative numerical integrals. A simple close-form solution for 'L' shaped current sheets was developed (Chen *et al.*, 2002), but the interaction force expressions of multi-pair of PM arrays or multi-pair of PM rings still have not been discussed. In order to obtain a complete panorama for better understanding, the development of a simple but accurate analytical solution becomes imperative for PM bearings.

In this study, a new analytical solution based on the current sheet model is presented. This analytical solution could be used in the magnetic force calculation of single- and multi-pair of PM rings or PM arrays. On the basis of the analytical solution, the characteristics of a novel PM thrust bearing are studied. In the proposed configuration, the rotor

‡ Corresponding author

* Project (No. 2006AA05Z201) supported by the National Hi-Tech Research and Development (863) Program of China

consists of stacked PM rings with alternative axial magnetization directions, while the stator with alternative radial magnetization directions, and copper rings are used to separate the adjacent PM rings. Finally, the performance of the PM thrust bearing is validated by the FEA method and experiments.

MATHEMATICAL MODELS

The current sheet model is commonly used in PM motor designs (Tang, 2005). It could be very convenient and fruitful for certain high-symmetry situations, such as radially and axially magnetized cylindrical annular rings (Leupold, 1993).

According to the current sheet concept, each element inside a uniformly magnetized PM has the identical magnetization intensity. Consequently, as shown in Fig.1, the equivalent current density inside the PM is zero, and non-zero only on the surface of the PM. So the surface equivalent current density $\boldsymbol{J}_s$ could be expressed as

$$\boldsymbol{J}_s = \frac{\boldsymbol{M}_r \times \boldsymbol{n}}{\mu_r}, \tag{1}$$

where $\boldsymbol{M}_r$ is the magnetization vector, $\boldsymbol{n}$ is the normal unit vector, and μ_r is the relative permeability of the PM.

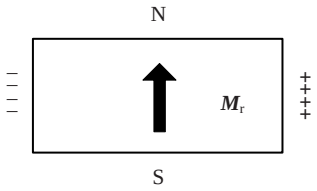

Fig.1 Current sheet model of the permanent magnet

Assumptions and simplifications

To develop a simple and accurate mathematical model, the following assumptions are made:

Assumption 1 The curvature of the structure is neglected; i.e., the gap between the PM rings is very small in comparison to their radius.

Assumption 2 The end magnetic field has no significant effect on the magnetic field; i.e., the lengths of PM arrays (vertical to their cross section) or the circumferences of PM rings are much larger than the gap.

Under such conditions, the 3D magnetostatic fields of PM rings or PM arrays could be modeled as a 2D magnetostatic one. We need only to analyze the array of infinite long bar-shaped PM arrays rather than the practical PM rings or PM arrays. The magnetic force could be easily converted according to the practical lengths of the PM arrays or PM rings.

Based on the aforementioned current sheet model and assumptions, the magnetic field and force of a novel PM thrust bearing are analyzed; its configuration is shown in Fig.2a. In the proposed configuration, the rotor consists of stacked PM rings with alternative axial magnetization directions, while the stator with alternative radial magnetization directions and copper rings are used to separate the adjacent PM rings. For convenience, here the axial direction is defined as the *Z* direction and the radial direction is defined as the *R* direction.

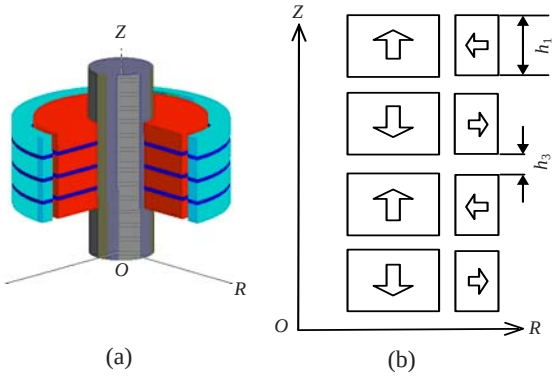

Fig.2 (a) Configuration of the proposed PM thrust bearing; (b) Stacked PM rings with alternative magnetization directions

One pair of magnets

According to the current sheet model, the magnetic field of one pair of magnets is equivalent to the magnetic field of two pairs of current sheets.

Fig.3 shows the cross section of one pair of magnets, and the dimension parameters. h_1 and h_2 are axial lengths of the stator magnet and rotor magnet, respectively; b_1 and b_2 are radial lengths of the stator magnet and rotor magnet, respectively. The displacement between the center lines of the rotor magnet and stator magnet is defined as *D*. The influence of the stator magnet on the rotor magnet could be separated by using equivalent magnets 1, 2 and 3. Among these equivalent stator magnets, magnets 1 and 2 provide *Z*-directional magnetic forces while magnet 3 produces *R*-directional magnetic force.

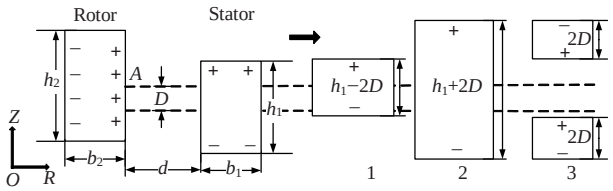

Fig.3 Equivalent magnetic array of one pair of magnets

Since all of the equivalent stator magnets are symmetric with respect to the center line of the rotor magnet, it is convenient to formulate the analytical solution of the magnetic field on point *A* (the crossing point of the rotor center line and positive current sheet). According to the Biot-Savart law, the magnetic induction intensity B_A could be expressed as

$$B_A=\frac{\mu_0 H_{c1}}{2\pi}\left[\left(\arctan\frac{b_1+d}{h_1/2-D}+\arctan\frac{b_1+d}{h_1/2+D}\right)-\left(\arctan\frac{d}{h_1/2-D}+\arctan\frac{d}{h_1/2+D}\right)\right]. \quad (2)$$

In Eq.(2), H_{c1} is the coercive force of the stator magnet, and μ_0 is the permeability of vacuum. The relative permeability of PMs is regarded as 1. The magnetic induction intensity at other points of the rotor's positive current sheet could be expressed in a similar way (only *D* is different).

So, the axial magnetic force F_{z1} on the rotor's positive current sheet, which is produced by the equivalent stator magnets 1 and 2, could be derived as

$$F_{z1}=F_1+F_2=F_0(E_1-E_2+E_3-E_4+E_5-E_6), \quad (3)$$

$$E_1=(h_1+D_1)\left(\operatorname{arccot}\frac{h_1+D_1}{b_1+d}-\operatorname{arccot}\frac{h_1+D_1}{d}\right), \quad (4)$$

$$E_2=(h_1-D_2)\left(\operatorname{arccot}\frac{h_1-D_2}{b_1+d}-\operatorname{arccot}\frac{h_1-D_2}{d}\right), \quad (5)$$

$$E_3=(h_1+D_2)\left(\operatorname{arccot}\frac{h_1+D_2}{b_1+d}-\operatorname{arccot}\frac{h_1+D_2}{d}\right), \quad (6)$$

$$E_4=(h_1-D_1)\left(\operatorname{arccot}\frac{h_1-D_1}{b_1+d}-\operatorname{arccot}\frac{h_1-D_1}{d}\right), \quad (7)$$

$$E_5=\ln\frac{[(b_1+d)^2+(h_1+D_1)^2][(b_1+d)^2+(h_1+D_2)^2]}{[(b_1+d)^2+(h_1-D_2)^2][(b_1+d)^2+(h_1-D_1)^2]}\cdot(b_1+d)/2, \quad (8)$$

$$E_6=\frac{d}{2}\ln\frac{[d^2+(h_1+D_1)^2][d^2+(h_1+D_2)^2]}{[d^2+(h_1-D_2)^2][d^2+(h_1-D_1)^2]}, \quad (9)$$

where $F_0=\mu_0 H_{c1}H_{c2}/(2\pi)$, H_{c1} and H_{c2} are the coercive forces of the stator and rotor magnets, respectively, and $D_1=h_2/2-D$, $D_2=h_2/2+D$.

Eqs.(3)~(9) also could be used to calculate the axial magnetic force on the rotor's negative current sheet when the air gap *d* is changed to $d+b_2$ and the force direction is opposite. Usually b_2 is much larger than *d*, so this force sometimes could be ignored.

Multi-pair of magnets

Based on the above analysis, when the single rotor magnet is near to the center line of the stator magnets, the axial force on the rotor's positive current sheet can be determined by superposition. That is to say, N_s pairs of stator current sheets have an impact on the rotor's positive current sheet. Here N_s is defined as the number of stator magnets, and N_r is the number of rotor magnets. The force expressions are similar to Eqs.(3)~(9). The only difference is that the dimension parameter h_1 will be replaced by h_n, as shown in Eq.(10), and the force directions will change alternately.

$$h_n=\frac{1}{2}\left[\left(n-\frac{1}{2}\right)(h_1+h_3)+\frac{1}{2}(-1)^n h_3+\frac{1}{2}(-1)^{n+1}h_1\right]. \quad (10)$$

To evaluate the effect of the stator magnets on the non-central rotor magnets, one needs to determine the influence of symmetrical and asymmetrical stator magnets arrays. The axial force expressions produced by symmetrical stator magnets arrays are similar to Eqs.(3)~(9). And for asymmetrical stator magnets arrays, only half the axial force will be produced. The fact that the polarities of every two neighboring stator magnets are opposite also should be considered. So the total magnetic force F_Z produced by the stator magnets on the rotor magnets is derived as

$$F_Z=\sum_{j=1}^{N_r}\left(F_0\sum_{n=1}^{2j-1}(-1)^m(E_{n1}-E_{n2}+E_{n3}-E_{n4}+E_{n5}-E_{n6})+\frac{F_0}{2}k_j\sum_{n=2j}^{2N_s-2j+1}(-1)^m(E_{n1}-E_{n2}+E_{n3}-E_{n4}+E_{n5}-E_{n6})\right). \quad (11)$$

In Eq.(11), m=int((n−1)/2), which means the round number of (n−1)/2. If j=(N_s+1)/2, k_j=0; otherwise, k_j=1, and if j>(N_s+1)/2, replace j by N_s+1−j.

$$E_{n1}=(h_n+D_1)\left(\operatorname{arccot}\frac{h_n+D_1}{b_1+d}-\operatorname{arccot}\frac{h_n+D_1}{d}\right), \quad (12)$$

$$E_{n2}=(h_n-D_2)\left(\operatorname{arccot}\frac{h_n-D_2}{b_1+d}-\operatorname{arccot}\frac{h_n-D_2}{d}\right), \quad (13)$$

$$E_{n3}=(h_n+D_2)\left(\operatorname{arccot}\frac{h_n+D_2}{b_1+d}-\operatorname{arccot}\frac{h_n+D_2}{d}\right), \quad (14)$$

$$E_{n4}=(h_n-D_1)\left(\operatorname{arccot}\frac{h_n-D_1}{b_1+d}-\operatorname{arccot}\frac{h_n-D_1}{d}\right), \quad (15)$$

$$E_{n5}=\ln\frac{[(b_1+d)^2+(h_n+D_1)^2][(b_1+d)^2+(h_n+D_2)^2]}{[(b_1+d)^2+(h_n-D_2)^2][(b_1+d)^2+(h_n-D_1)^2]}\cdot(b_1+d)/2, \quad (16)$$

$$E_{n6}=\frac{d}{2}\ln\frac{[d^2+(h_n+D_1)^2][d^2+(h_n+D_2)^2]}{[d^2+(h_n-D_2)^2][d^2+(h_n-D_1)^2]}. \quad (17)$$

In the final expressions Eqs.(11)~(17), there are no complicated and iterative numerical integrals; only an inverse trigonometric function and a logarithmic function are involved. So it is easier for researchers to analyze and design the PM bearings.

APPLICATION AND VALIDATIONS

Prototype design and construction

As the proposed analytical solution contains almost all the dimension and material parameters of the PM bearing, it is easy to optimize the parameters of the PM thrust bearing. The layer number (magnet pairs), N (N=N_s=N_r), is a critical parameter in the design when the total axial length of the PM bearing is fixed (Moser *et al.*, 2006). As shown in Fig.4a, the optimal layer numbers could be found at different air gaps when the total axial length of the PM thrust bearing is 12 cm. The numerical results have also revealed that parameter h_3 (the thickness of the copper rings) has little impact on the axial force if the dimension parameters are well designed, like h_1=10 mm (Fig.4b). Therefore, the copper rings could be used to reduce the demagnetization effect without thrust reduction, which resulted from the repelling phenomenon (Ohji *et al.*, 2000). A promising byproduct of the copper rings is that they also act as passive dampers to improve the rotation stability by means of their eddy current loss (Sung *et al.*, 2003).

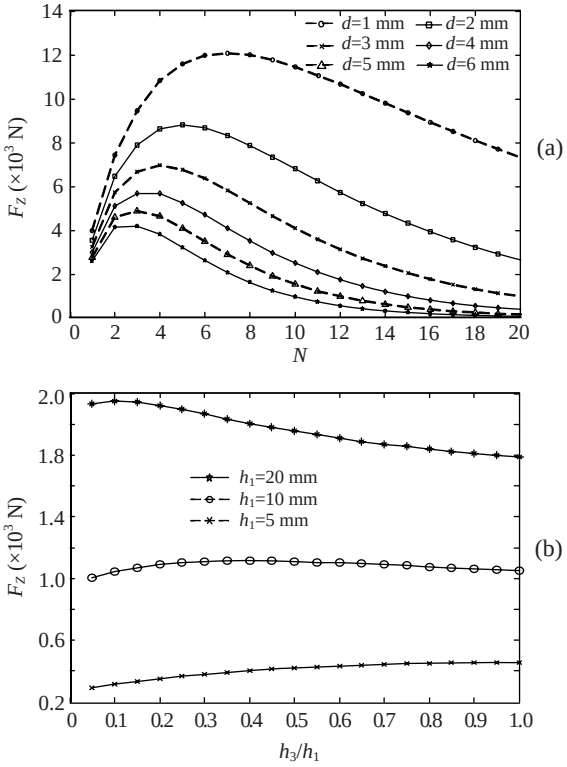

Fig.4 (a) Relationship between the axial force and the layer number when the total axial length of the PM thrust bearing is 12 cm; (b) Relationship between the axial force and h_3/h_1

d: air gap, h_1: axial length of the stator magnet, h_3: thickness of the copper ring, N: layer number

Using the above mentioned results, a prototype PM thrust bearing has been designed and built to support a composite flywheel. As shown in Fig.5, the PM thrust bearing is used to support all of the weight of the flywheel. The upper end of the rotor is restricted by an annular ball bearing, and the other end is connected to the adjustable speed motor by a flexible coupling. Table 1 lists the dimension and material parameters of the prototype PM thrust bearing.

Simulation results and numerical comparisons

To demonstrate the effectiveness of the present work, the thrust characteristics of the prototype PM thrust bearing were numerically studied by using the

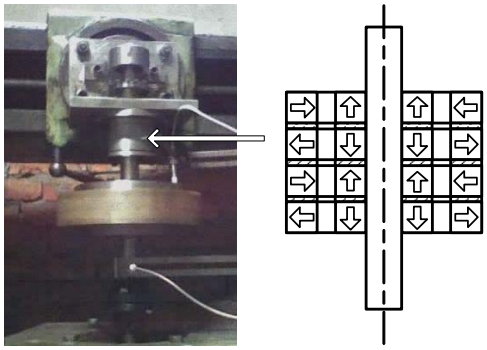

(a) (b)

Fig.5 Prototype (a) and configuration (b) of the PM thrust bearing

Table 1 Dimensions and materials of the thrust PM bearing

Part	Dimension (mm)	Material
Stator PM ring	Φ80×Φ70×10	NdFeB PM
Rotor PM ring	Φ64×Φ24×10	NdFeB PM
Shaft	Φ24	Stainless steel
Stator copper ring	Φ80×Φ70×2	Copper
Rotor copper ring	Φ64×Φ24×2	Copper

proposed analytical solution and FEA. The 2D and 3D FEA were realized by using software Maxwell 2D™ and Maxwell 3D™, respectively. For the analytical solution and 2D FEA, the 2D model considers the array of bar-shaped magnets and the 3D model considers the practical magnetic rings. Fig.6 gives the comparison of the axial forces obtained by using the two approaches. As shown in Fig.6, when the stator magnets and rotor magnets are in one-to-one correspondence (D=0), the axial force reaches its maximal value, and the variation of the axial force with the displacement in the axial direction follows a quasi-sinusoidal pattern. Subsequently, the area that has a positive axial stiffness can be found. For example, the reasonable working area for the PM thrust bearing in Fig.6 will be about 0~6 mm displacement in the axial direction. In this area, the PM thrust bearing is self-adaptive to the small change in the weight of the rotor or the axial disturbance.

According to the 2D FEA results, when D=0 the array of magnetic rings produces only axial forces, and there is no radial force on the surface of the magnetic rings. In case of $D\neq0$, the total radial force is still zero, but each part on the surface of the rotor magnets is under non-zero radial stress, which means

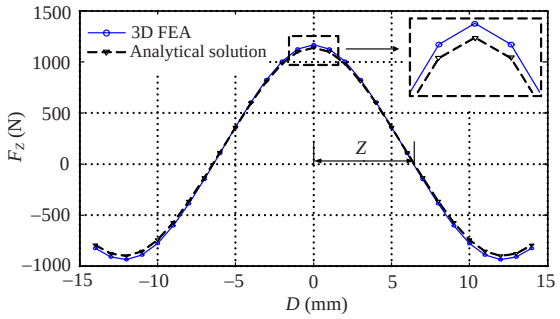

Fig.6 Force vs displacement in axial direction

that the rotor is in a state of critical balance in the radial direction. Only when there is a rotor eccentricity, will the total radial force exist.

According to the analytical solution, the maximal thrust in the axial direction is 1141 N, and the maximal thrust is 1168 N according to 3D FEA. As shown in Fig.6, the numerical results obtained from the proposed analytical solution show good agreement with those of 3D FEA. Consequently, the two assumptions seem reasonable and the accuracy of the proposed analytical solution has been confirmed.

Experimental study and validation

To further validate the proposed work, an experimental study was conducted on the prototype. In the experimental study, the prototype was installed on an upright drill. A Φ230 mm composite flywheel was connected to the rotor magnets through the shaft. The lower end of the rotor was connected to a 3 kW adjustable speed induction motor by using a flexible coupling. A 19-tooth non-uniform-pitch gear wheel and a photoelectric switch were used for speed measuring and rotor positioning. Two eddy-current sensors were used to measure the vibration characteristics of the PM thrust bearing. A spring balance was used to measure the static axial thrust. Under such conditions, the measured maximal static axial force was 1166 N with a 2% error.

The vibration characteristics of the prototype under different speeds were extensively tested, and the corresponding results are shown in Fig.7. CH1 shows the measured vibration characteristics of the PM thrust bearing at about 700 and 3500 r/min, which means the vibration of the flywheel is always less than 0.2 mm; CH2 shows the measured signal of the photoelectric switch. Again, these experimental results confirm the effectiveness of our model.

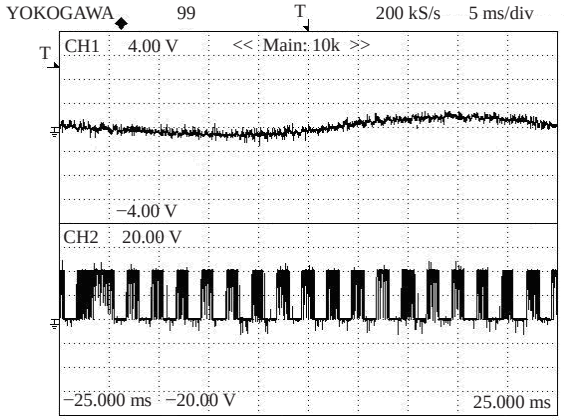

(a)

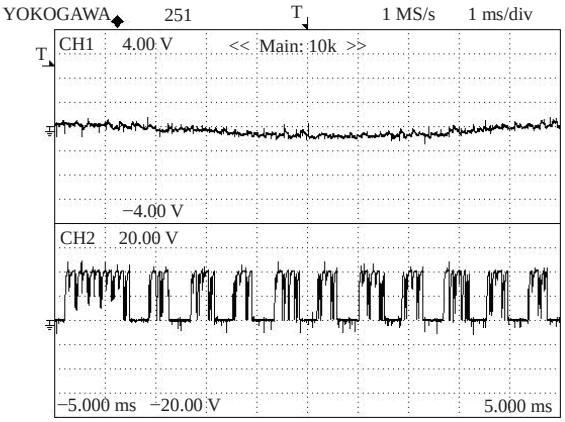

(b)

Fig.8 Vibration characteristics of the PM thrust bearing
(a) 700 r/min; (b) 3500 r/min

CONCLUSION

A new analytical solution based on the current sheet model is derived and a novel PM thrust bearing configuration is proposed. The new analytical solution is physically more intuitive and convenient for engineering designers than the traditional methods. The thrust characteristics of the proposed PM thrust bearing are extensively studied by using both the proposed analytical solution and finite element analysis. Finally, a prototype of PM thrust bearings is constructed and its static and dynamic performances are validated by experiments. The flywheel supported by the proposed PM thrust bearing spins stably at low and high rotation speeds.

Because the traditional thrust bearings have smaller thrust and stiffness, the proposed PM thrust bearing may have potential in many industrial applications. Moreover, the high speed test and the optimization design of the proposed PM thrust bearing will be the topics of further study.

References

Bancel, F., Lemarquand, G., 1998. Three-dimensional analytical optimization of permanent magnets alternated structure. *IEEE Trans. Magn.*, **34**(1):242-247. [doi:10.1109/20.650248]

Chen, C., Paden, B., Antaki, J., Ludlow, J., Paden, D., Crowson, R., Bearnson, G., 2002. A magnetic suspension theory and its application to the HeartQuest ventricular assist device. *Artif. Organs*, **26**(11):947-951. [doi:10.1046/j.1525-1594.2002.07125.x]

Leupold, H.A., 1993. Approaches to permanent magnet circuit design. *IEEE Trans. Magn.*, **29**(6):2341-2346. [doi:10.1109/20.280860]

Moser, R., Sandtner, J., Bleuler, H., 2006. Optimization of repulsive passive magnetic bearings. *IEEE Trans. Magn.*, **42**(8):2038-2042. [doi:10.1109/TMAG.2005.861160]

Mukhopadhyay, S.C., Ohji, T., Iwahara, M., Yamada, S., 2000. Modeling and control of a new horizontal-shaft hybrid-type magnetic bearing. *IEEE Trans. Ind. Electr.*, **47**(1):100-108. [doi:10.1109/41.824131]

Ohji, T., Mukhopadhyay, S.C., Iwahara, M., Yamada, S., 2000. Performance of repulsive type magnetic bearing system under non-uniform magnetization of permanent magnet. *IEEE Trans. Magn.*, **36**(5):3696-3698. [doi:10.1109/20.908944]

Sun, L.J., Zhang, T., Zhao, B., 2005. Study of mathematical model of permanent magnet bearings. *Chin. J. Mech. Eng.*, **41**(4):69-74 (in Chinese). [doi:10.3901/JME.2005.04.069]

Sung, T.H., Han, Y.H., Lee, J.S., Han, S.C., Jeong, N.H., Oh, K.S., Park, B.S., Oh, J.M., 2003. Effect of a passive magnetic damper in a flywheel system with a hybrid superconductor bearing set. *IEEE Trans. Appl. Supercond.*, **13**(2):2165-2168. [doi:10.1109/TASC.2003.813025]

Tang, R.Y., 2005. Modern Permanent Magnet Machines—Theory and Design. China Machine Press, Beijing, p.74-78 (in Chinese).

Xu, Y.L., Dun, Y.Q., Wang, X.H., Kong, Y., 2006. Analysis of hybrid magnetic bearing with a permanent magnet in the rotor by FEM. *IEEE Trans. Magn.*, **42**(4):1363-1366. [doi:10.1109/TMAG.2006.871396]

Yonnet, J.P., 1981. Permanent magnet bearings and couplings. *IEEE Trans. Magn.*, **17**(1):1169-1173. [doi:10.1109/TMAG.1981.1061166]